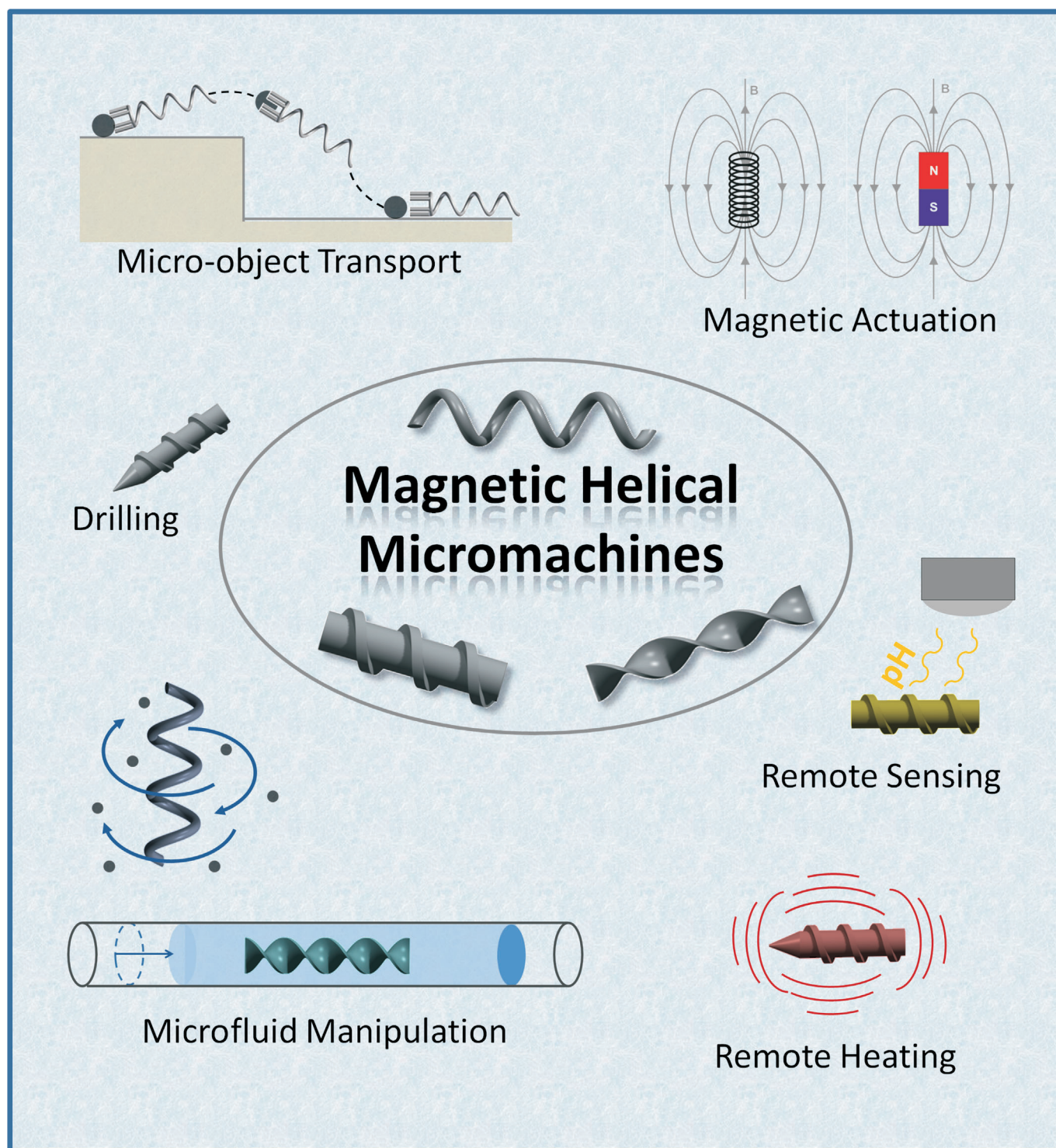


## Magnetic Helical Micromachines

Kathrin E. Peyer,<sup>[a]</sup> Soichiro Tottori,<sup>[a]</sup> Famin Qiu,<sup>[a]</sup> Li Zhang,<sup>[b]</sup> and Bradley J. Nelson<sup>\*[a]</sup>



**Abstract:** Helical microrobots have the potential to be used in a variety of application areas, such as in medical procedures, cell biology, or lab-on-a-chip. They are powered and steered wirelessly using low-strength rotating magnetic fields. The helical shape of the device allows propulsion through numerous types of materials and fluids, from tissue to different types of bodily fluids. Helical propulsion is suitable for pipe flow conditions or for 3D swimming in open fluidic environments.

**Keywords:** biomedical applications • drug delivery • magnetic actuation • magnetic properties • microrobotics

## Introduction

Magnetically actuated helical micromachines can be employed in a variety of biomedical applications, ranging from cell characterization in vitro, to in vivo diagnosis and therapy applications.<sup>[1]</sup> The main advantage of these helical micromachines lies in their ability to navigate in various types of fluid, ranging from water, blood, or urine, to more complex environments, such as cerebrospinal fluids, gastrointestinal tract, or brain matter. The actuation is applied by using low-strength rotating magnetic fields, which can be considered harmless to humans or other living organisms. Unlike other methods used for powering robotic devices, such as tethered devices or robots powered by onboard batteries, this wireless actuation method allows the miniaturization to the micro- and even nanoscale without any changes in the fundamental design approach. This makes magnetically actuated helical robots a promising tool for medical and biological tasks at various scales, reaching from the centimeter and millimeter range, for example, in medical treatment, to micro- and nanometer range for cell sorting and targeted delivery.

Magnetically steered helical microrobots for biomedical application have only been investigated for less than two decades. The first magnetically actuated helical prototype in the millimeter range was presented by Honda and co-workers<sup>[2]</sup> from Tohoku University in 1996 (see Figure 1). Their group published numerous papers showing the application of these helices or screw-type structures in muscle tissue or inside the gastrointestinal (GI) tract. Their publications

mainly focused on millimeter-sized prototypes in medical applications. Due to their main focus on the GI tract, no further miniaturization was attempted. It was only in 2007 that the first microscale prototype was successfully demonstrated by a group from ETH Zurich.<sup>[3]</sup> The main goal was shifted to magnetic actuation of micro- and nanoscale devices, and helical propulsion proved to be one of the most promising methods.<sup>[4]</sup> From that moment onwards, numerous groups have contributed to the research of magnetically actuated helical micromachines, albeit not all focusing on the same aspects of helical micromachines.

This article reports various magnetic helical micromachines that have the same fundamental propulsion mechanism. Specifically, they have a body-shape that transforms a rotation around their helical axis into a translational motion along the helical axis. The rotation is driven by an external rotating magnetic field, which applies a continuous torque to the device. The main areas of research with such helical micromachines can be categorized into four topics, namely actuation, motion control, fabrication, and functionalization. Each topic shall be elaborated separately in this article, starting with the propulsion mechanism and magnetic actuation methods. The subsequent section addresses the fabrication of micro- and nanoscale helical devices. The issues of non-ideal propulsion behavior and control strategies are discussed afterwards. The functionalization is closely related to the intended area of application and is discussed in the application section. Finally, the paper concludes with a summary and outlook on the topic of magnetic helical micromachines for biomedical applications.

## Propulsion Method and Magnetic Actuation

In this article we use the term “helical” device or robot for all the structures that transform a rotation around their helical axis into a translation along the helical axis. As mentioned previously, helical devices can be propelled in various environments and types of fluids. It is important to note that the physics behind propulsion of a screw in solid matter, along the walls of intestines, or in a viscous fluid environment are different. However, they all result in this type of motion, which will be referred to as “screw-type” motion. Figure 2 shows three basic shapes that are considered helical devices. They will be referred to as helix, screw, and twist in this paper. Depending on the type of motion needed for an application, a different robot shape may be chosen. A helix is characterized by a slender filament with a void center. A screw has a helical filament wound around a solid center. The third shape can be understood as a ribbon being twisted around its long axis. Figure 2 shows two prototypes, one at the millimeter and one at the micrometer scale, taken from literature for each category.

Helices (cork-screws) or screws are known for being used to drill into solid matter. When moving inside a solid-type

[a] K. E. Peyer, S. Tottori, F. Qiu, Prof. Dr. B. J. Nelson  
Institute of Robotics and Intelligent Systems  
ETH Zurich  
Tannenstrasse 3, 8092 Zurich (Switzerland)  
Fax: (+41) 44-632-1078  
E-mail: bnelson@ethz.ch

[b] Prof. Dr. L. Zhang  
Department of Mechanical and Automation Engineering  
The Chinese University of Hong Kong  
Shatin NT, Hong Kong SAR (China)



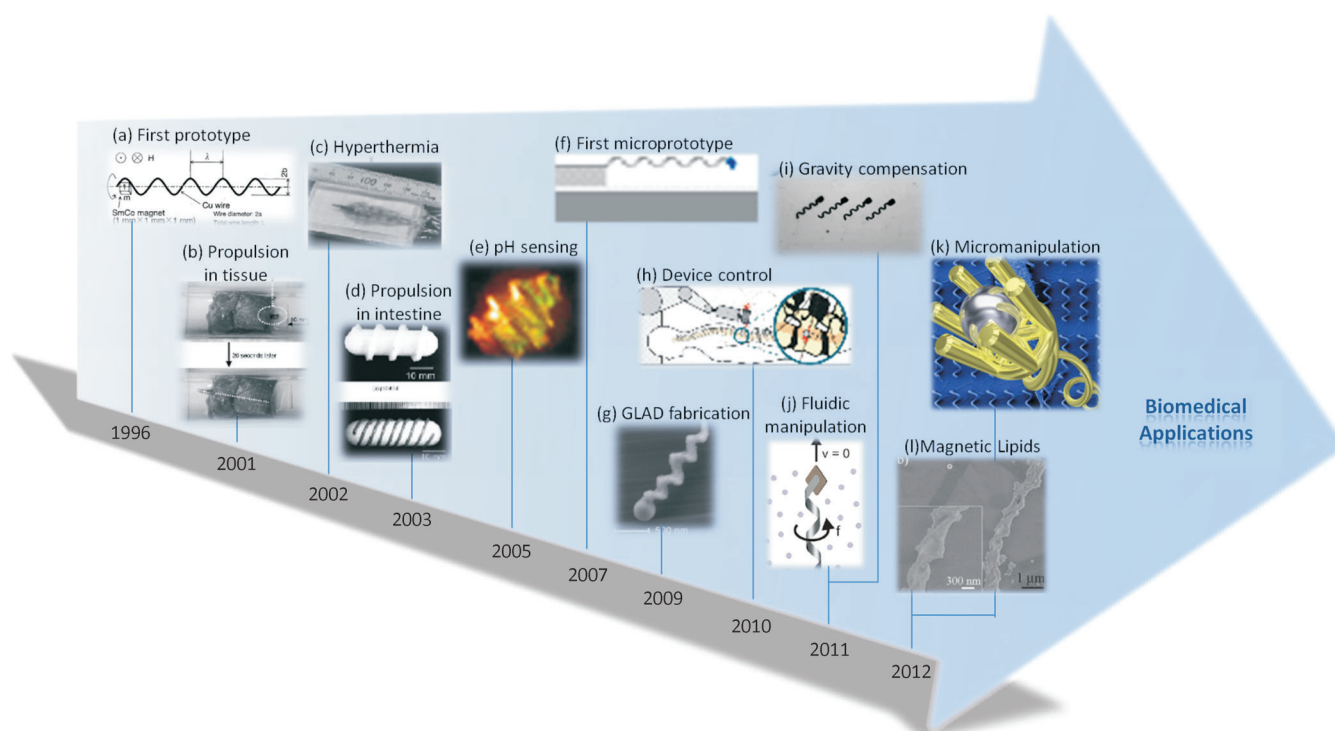


Figure 1. A history on magnetically actuated helical micromachines. a) First prototype suggested by Honda et al. in 1996.<sup>[2]</sup> b) Screw-type propulsion through tissue.<sup>[5]</sup> c) Hyperthermia.<sup>[6]</sup> d) Propulsion in bovine intestine.<sup>[7]</sup> e) Functionalization of the surface of helical machines—pH sensing using visual feedback.<sup>[8]</sup> f) First microscale helical device.<sup>[3]</sup> g) Glancing-angle deposition method for fabrication.<sup>[9]</sup> h) Non-uniform magnetic fields for actuation.<sup>[10]</sup> i) Gravity control algorithm.<sup>[11]</sup> j) Fluidic manipulation.<sup>[12]</sup> k) Micro-object transportation.<sup>[12]</sup> l) Lipid-based microhelix fabrication.<sup>[14]</sup> Parts a)–l) reused with permission.

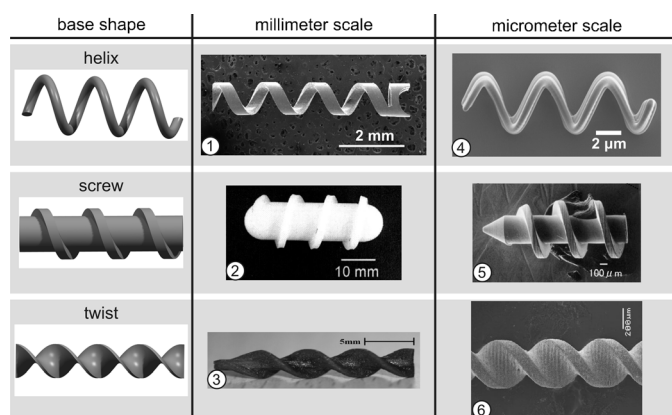


Figure 2. Basic shapes that can translate rotary to translation motion and vice versa at the millimetre (1–3) and the micrometre (4–6) scale. 1) Prototype for gravity compensation.<sup>[11]</sup> 2) Prototype for inside the intestines.<sup>[7]</sup> 3) Prototype for intravascular drilling.<sup>[15]</sup> 4) Polymer ABF presented by Tottori.<sup>[13]</sup> 5) Prototype for tissue drilling.<sup>[6]</sup> 6) Prototype for micro-fluidic pump.<sup>[16]</sup> Parts 1–3, 5, 6 reused with permission. Part 4 is a new SEM image of a polymer ABF used in reference [13].

material, helical shapes advance by one pitch per rotation. In this way, the rear part always moves into the same location at which the front part has already entered into the material. This motion is different in a soft environment, such as in the gastrointestinal tract or in a fluid environment. In order to characterize the motion of helices in fluids, it is im-

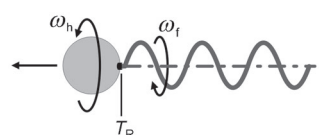
portant to look at the Reynolds ( $Re$ ) number at which they move. The  $Re$  number is a measure for the ratio of inertial versus viscous forces in a fluid and is defined as  $Re = UL\rho/\mu$ , in which  $U$  [ $\text{ms}^{-1}$ ] and  $L$  [m] are the velocity and characteristic length, and  $\rho$  [ $\text{kgm}^{-3}$ ] and  $\mu$  [Pas] are the density and viscosity of the fluid, respectively. For micro-structures or micro-organisms, both the characteristic length  $L$  and the velocity  $U$  are on the order of  $10^{-6}$ – $10^{-4}$  (in m or  $\text{ms}^{-1}$ , respectively), which results in a Reynolds number  $Re \ll 1$  in water. Motion at  $Re \ll 1$  can be best described like moving in a viscous medium, such as honey or tar. Humans would not be able to swim well in such an environment and micro-organisms have adopted alternative methods to move, such as using flexible beating flagella (e.g., spermatozoa) or rotating helical flagella (e.g., *E. coli* bacteria). A rotating helix can screw itself through the viscous environment, but, unlike a screw in solid matter, it slips and only advances by a small percentage of its pitch length per rotation. This seems to render the propulsion inefficient; however it is still one of the most well-suited swimming methods at low  $Re$  numbers and micro-organisms have to spend only a small fraction of their energy uptake on propulsion.<sup>[17]</sup>

Even more important is to evaluate the suitability of helical propulsion for man-made devices. There have been numerous approaches to use magnetic fields to actuate micro-devices.<sup>[18]</sup> Pure magnetic actuation is a promising method, because it is nontoxic to humans and other types of living

organisms. With magnetic fields it is possible to apply a force and a torque to a magnetized object. Abbott et al. presented a model that compared magnetic force-driven to torque-driven microrobots. The results showed that magnetic helical microrobots outperform force-driven microrobots in terms of maximum velocity and force generation when their size decreases to the micrometer scale.<sup>[4]</sup>

Bacteria have rotary motors<sup>[19]</sup> that apply a torque  $T_R$  to rotate their helical flagella at a frequency of  $\omega_f$ , which in turn induces a counter-rotation of their head at a low frequency  $\omega_h$  (see Figure 3a). Magnetically actuated helical mi-

(a) bacterial helical flagella propulsion



(b) helical micromachines propulsion

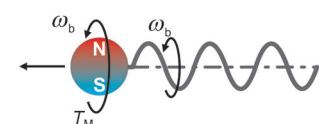


Figure 3. Actuation of helical flagella. a) Schematic of a bacterium, using an onboard rotary motor to actuate the helical tail. The torque  $T_R$  induces a rotation of the helical flagellum at frequency  $\omega_f$  (action), and a counter-rotation of the head at frequency  $\omega_h$  (re-action). b) A helical micromachine actuated with a magnetic torque  $T_M$ . It consists of a single rigid body, hence, the head and tail rotate with the same body frequency  $\omega_b$ .

comachines, on the other hand, do not have this counter-rotation between head and helical tail. A magnetic torque  $T_M$  is applied that rotates the whole rigid body with a frequency of  $\omega_b$  (see Figure 3b). A magnetized object in a magnetic field experiences a magnetic torque that acts to align the object's magnetization axis with the orientation of the magnetic field. This principle is known from a compass needle, which aligns itself with the earth's magnetic field. Once the axis is aligned, the torque vanishes and no further rotation is induced. In order to maintain a continuous rotation of the object, which is necessary for actuating helical micromachines, the magnetic field itself has to be rotated. Most commonly a helix is used for propulsion in a fluid, although screws and twists have been used as well (see section on Applications).

There are two ways to create an external magnetic field for helical micromachines actuation: either a strong permanent magnet or electromagnetic coils can be used. A permanent magnet has a fixed magnetization and in order to adjust the field strength and orientation the magnet has to be moved closer or further away and be rotated by using a motor. Electromagnetic coils generate a magnetic field by running current through the loops. In order to adjust the field strength only the amplitude of the current has to be changed and the coils do not have to be physically moved.

To create arbitrary rotating fields in three dimensions, three coil pairs can be placed orthogonal to each other and a sinusoidal alternating current applied (see Figure 4a and b).

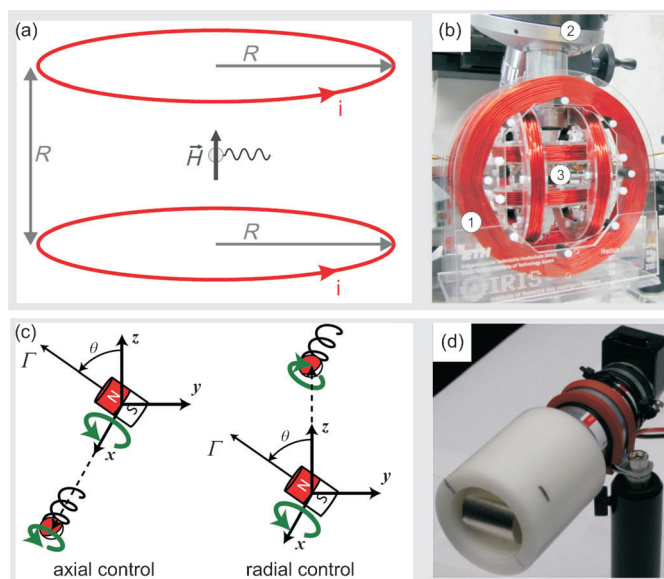


Figure 4. Magnetic field generation. a) Electromagnetic coil pair in a Helmholtz configuration.  $H$  represents the magnetic field [A m] generated by the coils. b) Experimental setup with three orthogonal Helmholtz coil pairs. c) Actuation through rotating a permanent magnet. The magnet can be placed in axial or radial direction with respect to the helical micromachine. d) Experimental setup with a permanent magnet rotated by a motor. Parts a)–c) reprinted with permission of Elsevier,<sup>[21]</sup> part d) reprinted with permission of IEEE.<sup>[10]</sup>

By placing the coils at a distance equal to their coil radius from each other, approximately uniform fields can be achieved in the center. This type of coil configuration is called a Helmholtz coil configuration and is beneficial for avoiding drift due to magnetic forces. Most experiments with helical micromachines have relied on the use of electromagnetic coil setups, and the majority of these use a Helmholtz coil configuration. More complex electromagnetic actuation systems, such as the OctoMag, which consists of eight solenoids and is designed for magnetically steering microdevices during eye surgery,<sup>[20]</sup> can also be used to actuate helical microdevices. Unless space requirements ask for these types of complex coil setups, Helmholtz coils are sufficient to actuate helical microrobots. In 2010 Fountain et al. showed how to use rotating permanent magnets to actuate helical micromachines in a controlled manner.<sup>[10]</sup> The rotating permanent magnet can either be aligned with the helical axis (axial control) or in the radial direction of the helix (radial control) as depicted in Figure 4c. Figure 4d shows an experimental setup with a permanent magnet rotated by a motor.

## Fabrication of Helical Microstructures

Initial helical microrobot designs presented in the literature were several millimeters in size.<sup>[2,22]</sup> There are several rea-

sons for this. First, there was a lack of suitable fabrication methods for the microscale then. Second, the intended purpose of the machine did not necessarily require a micro-sized design. And third, fundamental research could be done with up-scaled models, such as studying low *Re* number hydrodynamics by using highly viscous media instead of water. In recent years, magnetically actuated microrobots have become increasingly studied for use in biomedical applications, ranging from minimally invasive surgery, to targeted drug delivery, or cell manipulation.<sup>[1]</sup> As mentioned previously, it was shown that magnetically actuated helical propulsion is one of the most promising methods at the microscale.<sup>[4]</sup> At the microscale many fabrication methods rely on the deposition or removal of thin layers of material, which complicates the creation of complex 3D structures, such as a helix.

The first complete helical microrobot prototype, the artificial bacterial flagellum (ABF), was presented in 2007.<sup>[3]</sup> The fabrication was based on traditional thin-film deposition methods and monocrystalline thin-film growth. By depositing or growing, bi- or trilayers of material, internal stresses in the structure result in a bending of the thin films.<sup>[23,24]</sup> In this manner straight ribbon patterns can form helices in a controllable fashion (see Figure 5a).<sup>[25]</sup> By tuning the deposition parameters, such as the film thickness, the ribbon width, or the orientation of the ribbon with respect to the

crystalline structure of the metal, the curvature can be finely tuned. In 2007 Bell et al. reported the helix design including a soft-magnetic head for actuation.<sup>[3]</sup> Helical microrobots with diameters of around 3  $\mu\text{m}$  and variable tail lengths of 10–100  $\mu\text{m}$  were achieved. Like the schematic shown in Figure 3b, the ABFs have a non-magnetic helical tail with the magnetic material localized only in the head design. The swimming and actuation was explored in detail in further publications in 2009.<sup>[26]</sup>

In 2009, a publication by Ghosh and Fisher demonstrated the batch fabrication of helical microrobots by means of glancing-angle deposition (GLAD).<sup>[9]</sup> Spherical seeds are densely packed on the substrate, and pillars are grown at an oblique angle. By continuous rotation of the substrate, the pillars grow into a helical shape (see Figure 5b). These prototypes were even smaller, with a diameter of 500 nm and a length of 2–3  $\mu\text{m}$ . The magnetic material, that is, cobalt, was deposited on one side of the swimmer along the whole body length and was reported to be permanently magnetized in a radial direction. This process is still limited in the choice of shape parameters as well as the material selection.

In 2012 Tottori et al. presented a helical swimmer prototype fabricated by a 3D laser writing tool.<sup>[13]</sup> Direct laser writing (DLW) allows the creation of arbitrary 3D structures. A photoresist is deposited on a glass substrate, which can be moved in three dimensions with a piezoelectric stage.

At the focal point of the laser, two-photon polymerization (TPP) occurs and, after removal of the undeveloped negative photoresist, only the structure remains on the substrate (see Figure 5c). The magnetic material is deposited afterwards by means of electron beam evaporation on the entire helical structure. Other approaches have used magnetic microparticles inside the polymer.<sup>[27]</sup> The micrometer-sized particles increase the minimum feature size considerably and only a low concentration of particles can be used, because the polymerization is impaired due to the scattering of the laser beam.

For biomedical applications, such as targeted drug delivery, it is necessary to have suspensions of helical swimmers as drug carriers that can be directed into human bodies with a tunable dose. Recently, a simple and general method to obtain suspensions of helical swimmers was devel-

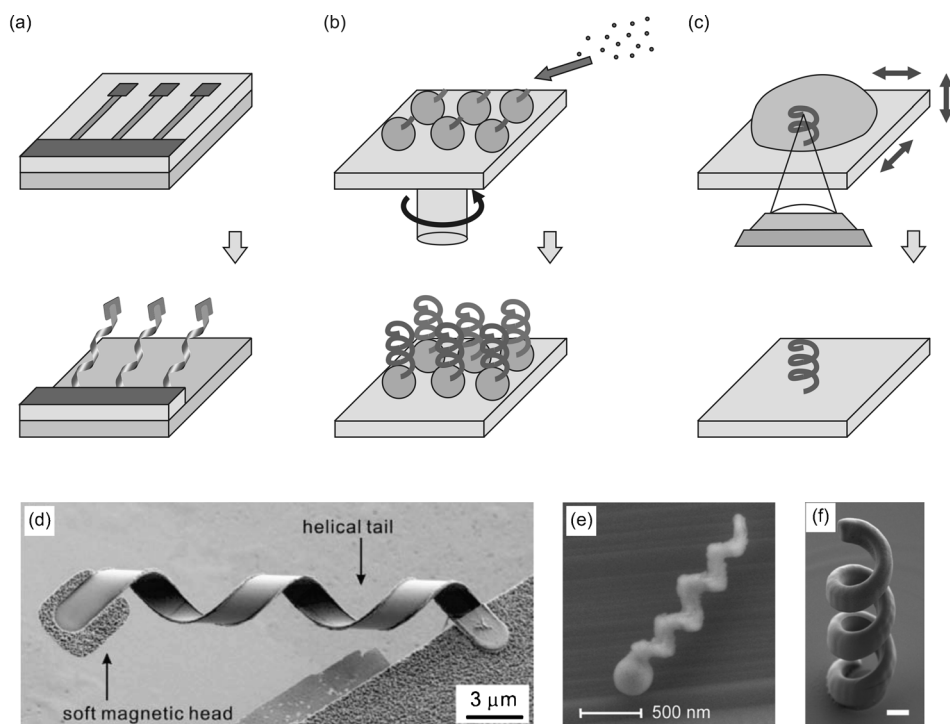


Figure 5. Fabrication methods. a)–c) Schematic representations of fabrication methods for creating micro-helices.<sup>[21]</sup> a) Self-scrolling technique: after release from the supporting layer, the thin bi- or trilayer ribbons scroll into helical shapes. b) Glancing-angle deposition (GLAD): deposition of pillars on spherical seeds from a steep angle. By rotating the substrate during the deposition, helical tails are created. c) Direct laser writing (DLW) for fabricating 3D structures into a photoresist by two-photon polymerization (TPP). Arbitrary structures can be programmed and fabricated. d)–f) Fabricated prototypes: d) Self-scrolled ABF.<sup>[26b]</sup> e) GLAD prototype.<sup>[9]</sup> f) DLW tool fabricated ABF.<sup>[13]</sup> The scale bar is 2  $\mu\text{m}$ . Parts a)–f) reused with permission.

oped using sonication.<sup>[9]</sup> Further investigation indicated that it is a nondestructive approach to release tethered helical device arrays from the substrate.<sup>[28]</sup> The schematic of the process flow to prepare suspension of helical devices is shown in Figure 6a. After sonication, suspensions of unteth-

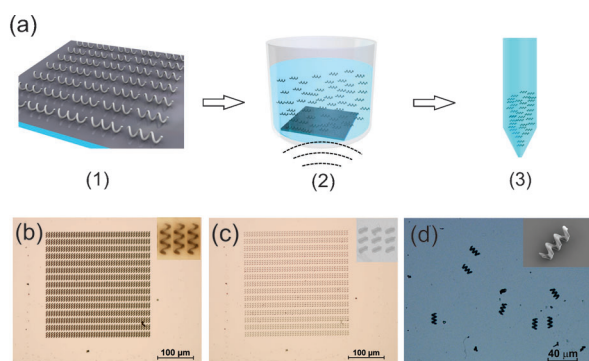


Figure 6. Suspension of helical micromachines. a) The schematic diagram of bath releasing process: 1) as-fabricated arrays of micromachines, 2) releasing microdevices from the original substrate by sonication in isopropyl alcohol, and 3) suspension of microswimmers. b) The optical image of the glass substrate before sonication, and the inset is a magnified optical image of b). c) The optical image of the glass substrate after sonication, the inset is a SEM image of c). d) The optical image of helical micromachines after one drop of suspension dried on a glass slice, the inset is a SEM image of one helical micromachine after sonication.

ered helical micromachines in different solutions can be collected by centrifugation. Figure 6b shows the tethered helices arrays before sonication, and Figure 6c shows that the helices are completely detached from the glass substrate after sonication. The sonication process does not impact the shape (see Figure 6d) and swimming performance of the devices.<sup>[28]</sup>

The fabrication of magnetic nanohelices based on lipid growth was demonstrated by Schuerle et al.<sup>[14]</sup> The growth of lipids can be influenced by the alcohol concentration in the solution, resulting either in helical or tubular (zero-pitch-helix) structures (see Figure 6a and b). Pd clusters are used for seeding (Figure 7b, step 1) and finally a magnetic CoNiReP coating is applied by using electroless deposition (Figure 7b, step 2). A helical magnetic prototype is shown in Figure 7c. In swim tests rotation around the helical axis and forward motion were demonstrated.

### Helical Propulsion and Motion Control

The optimal motion of a helical micromachine is a pure rotation around and a pure translation along its helical axis. A number of factors influence their motion. One phenomenon reported previously is the wobbling of helical swimmers at low frequencies (see Figure 8a). The helical tail has no axis of symmetry that naturally results in a slight wobbling motion, and additional asymmetric design features, such as the off-center attachment of a head, can enhance the wobbling.<sup>[29]</sup> Furthermore, the direction of magnetization of the

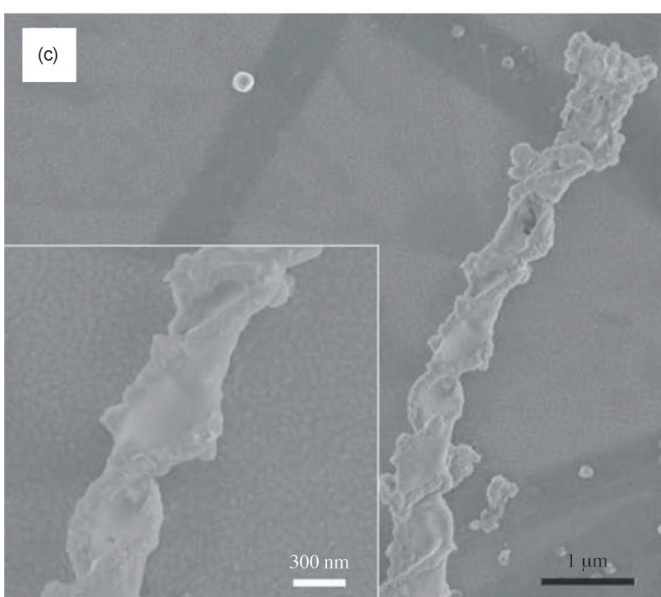
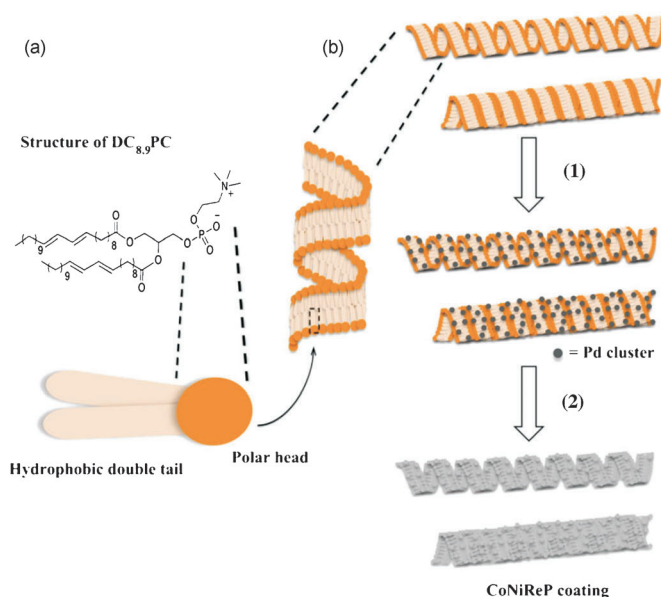


Figure 7. Magnetic nano-helix fabrication using lipids. a) and b) Lipids self-scroll into helices with various pitch values depending on the alcohol concentration. The magnetic CoNiReP is applied using electroless deposition. c) SEM image of a helical prototype. Reused with permission from reference [14].

swimmer plays a role in the alignment of the swimmer with respect to the helical axis.<sup>[13]</sup> It was demonstrated that the swimming stabilizes at high actuation frequencies (see Figure 8b).

A further aspect is swimming near a solid wall. The presence of a solid boundary increases the apparent viscosity of the fluid.<sup>[30]</sup> This leads to a drag imbalance on the helix resulting in a lateral force, which results in a drift motion perpendicular to the helical axis.<sup>[31]</sup> The total velocity is the addition of the forward velocity due to the helical propulsion and the drift velocity due to wall effects (see Figure 8c).



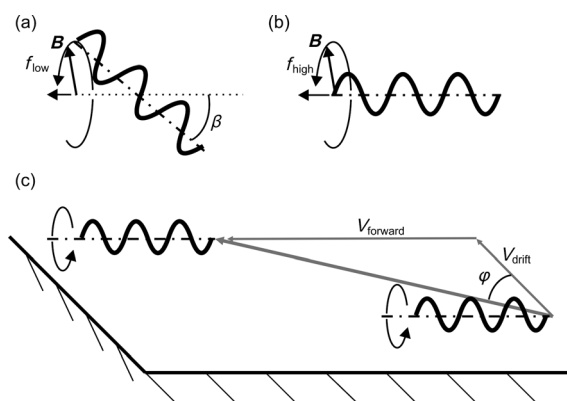


Figure 8. Motion of helical swimmers. a) At low frequencies the swimmer wobbles with a wobbling angle  $\beta$ . b) The wobbling decreases at high rotational frequencies. c) Motion near a solid wall. The swimmer "rolls" along the surface, resulting in a drift velocity in addition to the forward velocity.

This phenomenon is present for all types of low  $Re$  number locomotion near a solid boundary. For example, *E. coli* bacteria swimming near a glass substrate move in circles because of the counter-rotation of head and tail.<sup>[32]</sup> Some magnetic devices rely on these wall effects to achieve locomotion.<sup>[33]</sup> This type of motion is often referred to as tumbling or rolling and is characterized by a translation along the wall in the same plane as the rotation plane of the magnetic field. This is a promising method to create propulsion for lab-on-a-chip and in vitro applications. Unlike helical propulsion, however, tumbling only works near a solid boundary and does not allow free swimming in three-dimensions.

In addition, the influence of gravity has to be accounted for when actuating helical micromachines in a fluid. Micro-organisms consist mainly of water, which makes them nearly neutrally buoyant in water or fluids of a similar density. This is not generally true for helical micromachines. Despite there being several different types of materials that can be used for the microrobots, they are generally denser than water, especially the metallic components necessary for the magnetic actuation. If the microrobot has to swim in an open cavity, it has to compensate for the gravity or it will continuously drift downwards.<sup>[11]</sup> One approach to solve this problem is to implement a model-based algorithm that compensates the gravitational forces with the propulsive forces of the robot as shown in Figure 9. A helical swimmer can generate a propulsive force in the direction of the helical axis. By swimming at a pitch angle this propulsive force can be used to counteract the gravity. The pitch angle is dependent on the relative weight of the swimmer and its rotational frequency.

Finally, the environment can also influence the swim performance. Most microdevices are tested in water or other types of Newtonian fluids. Mahoney et al. showed that they can move screw-type swimmers in viscoelastic fluids with a similar property to brain matter.<sup>[34]</sup> They discovered a destabilizing torque acting on the device that needs to be accounted for when moving in this type of environment.

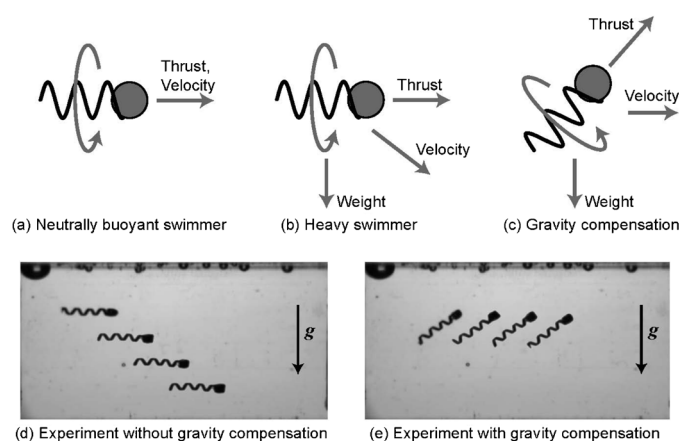


Figure 9. Gravity compensation. a) Motion of a neutrally buoyant swimmer. b) A heavy swimmer without gravity compensation drifts downwards. c) Gravity compensation through thrust generated by the helical swimmer. d) Experimental results without gravity compensation. e) Experimental results with gravity compensation. Parts a)–e) reused with permission from reference [11].

Bodily fluids contain cells and fibers that can also influence the swimming performance of helical micromachines. ABFs were successfully tested in solutions containing methyl cellulose fibers with viscosities higher than that of the human blood or the cerebrospinal fluid.<sup>[35]</sup>

## Functionalities and Biocompatibility

The applications areas of helical micromachines are as versatile as their shapes and sizes. These areas include a range of medical applications, for example, targeted delivery, hyperthermia, or ablation of tissue. Furthermore, there are numerous applications in biology, for example, in cell sorting or single-cell analysis. The basic helical micromachine designs must be functionalized in order to fulfill a specific task. Functionalization may occur through the addition of parts, for example, for micro-object transport, or by chemical surface treatment, for example, for remote sensing tasks.

One application of helical micromachines is for the precise transportation of cellular or subcellular objects. Several methods of transportation have been proposed and categorized.<sup>[1b]</sup> Mechanical transportation can be categorized into two types, that is, with physical contact or by using micro-fluidic flow induced by the microswimmer. As helical micromachines create thrust force along their helical axis when rotating, they are capable of pushing an object in front of them or towing an object attached at the back. Preliminary studies showing the capability of pushing 6  $\mu\text{m}$ -diameter polystyrene beads and 5  $\mu\text{m}$ -diameter silica beads were performed by the two groups that developed the ABFs.<sup>[9,26a]</sup> Due to the versatility of DLW, this type of micromanipulation was significantly improved by implementing handlike structures at one end of the helical structures.<sup>[13]</sup> As schematically shown in Figure 10a, the helical micromachine loads and transports the object by pushing and releases it by

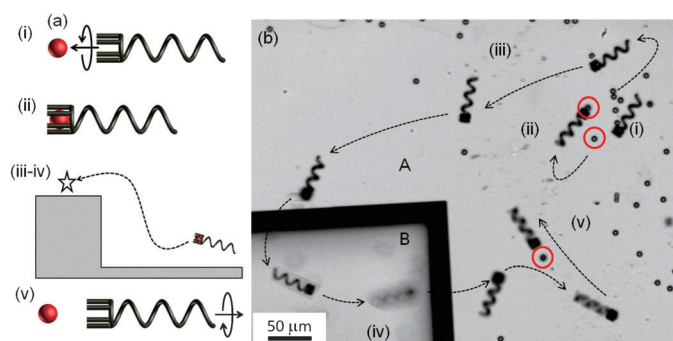


Figure 10. Contact manipulation. a) Schematic illustration of pick-and-place manipulation: i) approaching, ii) loading, iii) and iv) transporting, and v) releasing. b) Time lapse image of pick-and-place manipulation. Reused with permission from reference [13].

swimming backwards. Once the particle slips into the holder, it is not dislodged even when the ABF swims in three-dimensions due to the flow surrounding the ABF. Releasing is performed simply by rotating the ABF inversely. Figure 10b shows the time lapse image of the pick-and-place manipulation. The handlike structures themselves are rigid and do not close and re-open. More functional units might help enhance the dexterity of manipulation with the helical micromachines.<sup>[36]</sup> By using the propulsion force, the helical micromachines are also capable of towing objects. For example, wire trailing by using helical micromachines was demonstrated in viscous silicone oil.<sup>[37]</sup> The wire was trailed and steered at the branch of the millimeter-scale channels. Penetration and drilling require greater thrust than transportation of cargos, because the surfaces of tissues or cell membranes have to be mechanically opened. Drilling into agar and bovine tissues was performed at the millimeter scale using screw-type micromachines.<sup>[5]</sup> As described in the section “Propulsion Method and Magnetic Actuation”, screw-type devices are propelled in a different manner than helical swimming robots. They drill the tissue by using their sharp tips at the front and propel by the mechanical friction between the drill and tissue. Permanent magnets, typically NdFeB magnets, were used for both drill-like micromachines and endoscopic helical micromachines, since a large torque is required to overcome the mechanical friction from the environment.

Common challenges for lab-on-a-chip applications are the mixing and pumping of minute fluid quantities. By propelling through liquid, the swimmers influence the fluid surrounding them. Instead of placing the emphasis on the motion of the device, the reaction of the fluid to their motion can be employed for pumping. For example, a twist-shaped microrobot (see Figure 2) was employed to pump fluid inside a capillary. The robot was kept stationary by applying a magnetic force opposite to the propulsive force generated by the swimmer.<sup>[16,27]</sup> It was shown that bacteria can be used for pumping and mixing fluids<sup>[31,38]</sup> as well as for the transport of micro-objects.<sup>[39]</sup> However, bacteria need an environment that provides nutrition and is kept at moderate temperatures. This disadvantage can be overcome

by using artificial helical micromachines. As they mimic the propulsion method of bacteria, they also exhibit a similar pumping effect in the fluid. The pumping of a single micro-robot is local, acting mostly along the length of the helical swimmer and dissipating quickly in front and behind the microrobot.<sup>[12]</sup> This can be useful as the helical micromachine can act as a remotely controlled mobile micropump. In this way micro-objects can be transported in a contact-free manner, which is beneficial if sensitive material, for example, a cell, is to be moved. Figure 11a shows initial results

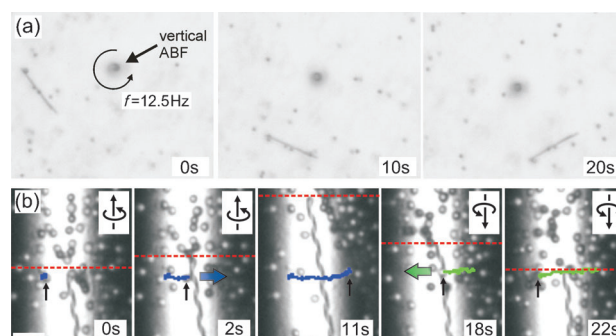


Figure 11. Noncontact manipulation. a) Contact-free rotation of a micro-needle. b) Reversible pumping of micro-beads. The ABF moves forward for the first 11 s then reverses its direction of motion. The blue and green line tracks the motion of a single microbead during forward and backward motion, respectively. Scale bar corresponds to 10  $\mu\text{m}$ . Reused with permission from reference [12].

rotating a micro-spike without contact with the helical micromachine. The motion as well as the pumping direction can be reversed simply by reversing the rotation of the magnetic field (see Figure 11b). A different approach to micro-manipulation is the use of chemically fuelled devices that use magnetic fields only for steering. The transport and piercing of cells could be demonstrated successfully, however, the devices only move in an environment containing hydrogen peroxide, which creates a challenge for application in vivo.<sup>[40]</sup>

Since helical micromachines are wirelessly driven, sensing also needs to be performed wirelessly. At relatively large scales, such as the capsule endoscopic robots, the robots can have a camera, sensors, memory and transmitter on-board. The images taken inside the human body were sent to a receiver placed on the patient, or the images are stored and read out after the robots are extracted from the human body. However, as the size becomes smaller, conventional sensors and memory are not able to be integrated on the robots due to the limited size. A promising approach for remote sensing is the use of chemicals that respond to particular inputs, such as pH or temperature. For example, the surface of a screw-type robot was coated with a pH-responsive fluorescent material (see Figure 12).<sup>[8]</sup> On one side of the device the pH coating was intentionally deactivated in order to modulate and subtract background for processing the spectra data. The micromachines were able to screw through a gelatin environment with discontinuous pH



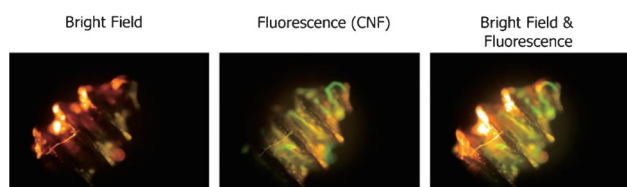


Figure 12. A helical micromachine for remote pH sensing using fluorescence. The top is coated with pH-sensitive fluorescence. Reused with permission from reference [8].

values, and measure the local pH value. Remote sensing by using fluorescence was also proposed for oxygen concentration measurements with other types of microrobots.<sup>[41]</sup>

Magnetic helical micromachines might significantly improve the quality of cancer therapy in the future by means of hyperthermia. Hyperthermia is a type of medical treatment intended to kill cancer cells by locally exposing them to high temperature (40–50 °C). One approach to remotely heat a device is through inductive heating by applying oscillating magnetic fields. In 2002, an induction unit for localized hyperthermia was mounted on a helical micromachine in order to add locomotive function.<sup>[22,42]</sup> The device consisted of a magnetic driller and the heating unit. Oscillating fields with field strengths of 6–8 mT and a frequency of 100 kHz were used to heat up the micromachine. The micromachine was driven by a rotating field with field strengths of 12–15 mT and in a frequency range of 1–10 Hz. Figure 13

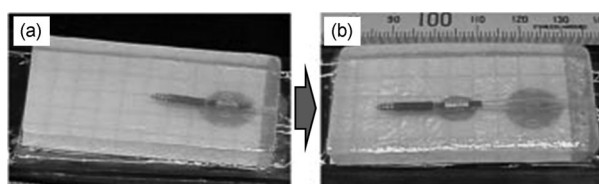


Figure 13. Inductive heating using oscillating fields. a) After heating for 20 min. b) After 7 min of locomotion and 10 min of heating. The gray patch indicates the location where the temperature is over 50 °C. Reused with permission from reference [42].

shows that the micromachine was first heated up using oscillating field for 20 min (see Figure 13a), afterwards it was driven using a rotating field for 7 min, and then it was heated up again at the new position for 10 min as shown in Figure 13b. The change of the color (gray scale in Figure 13) is from the thermosensitive sheet changing color at 50 °C under the agar. Scaling down the device to the micro/nano-scale is the next challenge. Thus far, the materials and fabrication methods of the helical micromachines are still limited, and their behavior in high oscillating fields for inductive heating are not yet well studied.

Biocompatibility and biodegradability of microdevices are other crucial factors that need to be taken into account for biomedical applications. Thus, they are expected to be fabricated from materials with low toxicity to cells and tissues. A common method to achieve this goal is to coat the surface

of micromachines with biocompatible materials such as titanium. Figure 14 shows mouse myoblast C2C12 cells lying on the horizontal arrays of helical devices with IP-L (a liquid negative photoresist by Nanoscribe GmbH) polymer bodies

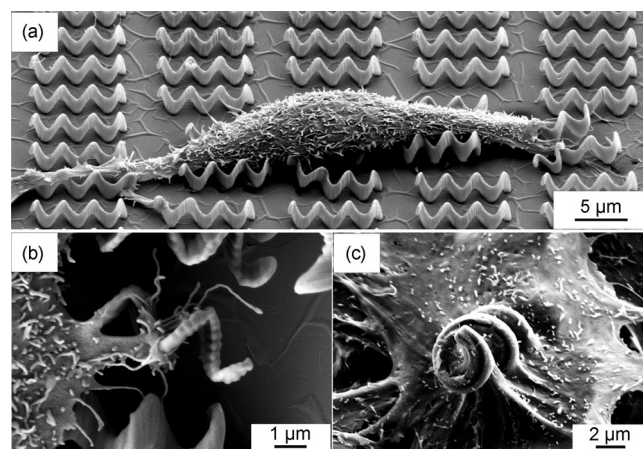


Figure 14. a) A mouse myoblast cells C2C12 lays on the arrays of helical micromachines with IP-L polymer bodies and Ni/Ti bilayer coating after 1 day culture. b) The C2C12 cell contacts with helical swimmers via lamellipodial and filopodial interactions. c) C2C12 cells contact with helical micromachines with SU-8 polymer bodies and Ni/Ti bilayer coating after 3 day culture. Reused with permission from reference [13].

fabricated with the DLW method with a Ni/Ti bilayer coated using e-beam deposition.<sup>[13]</sup> Figure 14b shows the cell contact with swimmers by means of lamellipodial and filopodial interactions in detail.<sup>[43]</sup> Helical microswimmers with other polymer materials such as SU-8, an epoxy-based negative photoresist by MicroChem (see Figure 14c), and Ormocomp, a commercial biocompatible photosensitive resin, were also studied. For long-term biocompatibility, iron-based magnetic helical devices are envisioned. It was reported that iron has a high degree of biocompatibility as a stent material in animal tests.<sup>[44]</sup>

## Summary and Outlook

Magnetically actuated helical micromachines are versatile tools for biomedical applications (Figure 15). The main research challenges can be categorized in terms of fabrication, actuation, control, and functionalization. Numerous successful approaches have been presented for the fabrication of helical micro- and nanostructures. Two actuation methods have been proposed in the literature, that is, the use of stationary electromagnetic coils or the use of rotating permanent magnet. The strength of the magnetic field generated by electromagnetic coils can be easily adjusted by tuning the amount of current running through the coils. The challenge lies in the design of coils that can create strong enough magnetic fields while being arranged optimally near the work space. Rotating permanent magnets are more difficult to control as the actuation field is highly nonlinear. Their ad-

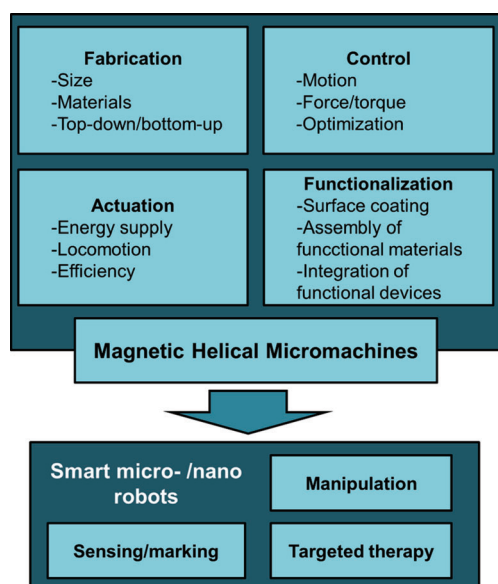


Figure 15. A roadmap for magnetic helical microrobots for biomedical applications.

vantage lies in the strength of the magnetic field that can be reached for a magnet of relatively small dimensions. If combined with a robotic arm that can change the position of the permanent magnet, this approach also shows promise in medical applications.

There are two basic requirements in order to be able to implement advanced motion control. First, the modeling of the motion of helical devices is crucial. At the time when helical micromachines were introduced, detailed studies on helical locomotion had already been published.<sup>[45]</sup> This was because the motion of micro-organisms using helical propulsion had been investigated by biologists and researchers with a background in theoretical fluid dynamics. Unlike their natural swimming counterparts, helical microrobots receive their power from an external source. These new aspects of helical propulsion are ongoing topics of research. The second requirement for motion control is the ability to track the microrobot. Current approaches rely mostly on optical feedback with a microscope and camera. This is sufficient for many types of applications, but poses a challenge for maneuvering inside most areas of the human body. Other means of tracking, for example, ultrasound, magnetic resonance imaging, and fluorescence imaging are still to be investigated.

Finally, the broadest area of research is the functionalization of helical microrobots. One of the basic features that most devices will have to incorporate is biocompatible materials. For various applications it may be sufficient to functionalize only the surface of the device. For others, it is expected that biocompatible or biodegradable material has to be used for the majority of the device. Other types of functionalization are as diverse as the potential type of applications. They can be broadly described as mechanical functionalities and chemical functionalization. An example for a

mechanical function is the addition of a claw for enhanced transport of micro-objects such as presented by Tottori et al.<sup>[13]</sup> Chemical functionalization may include a fluorescence coating or other types of smart materials that can respond to external stimuli. Hydrogels are smart polymers that have been extensively studied as smart drug-release systems.<sup>[46]</sup> Bilayered hydrogels or other types of polymers can also respond with a shape change to different chemical environments.<sup>[47]</sup> The discussion of the extensive research area of smart polymers is, however, beyond the scope of this article. A major goal is the application of helical microrobots for targeted drug delivery. This complex application combines most of the challenges discussed previously. It requires the tracking of the microrobots in the human body, they have to be biocompatible if not biodegradable, and they have to be functionalized to be able to transport drug payload.

The development of magnetic helical micromachines is a fascinating field of research, and these types of remotely controlled devices have great potential to be employed in a variety of biomedical applications at the millimeter, micrometer, and nanometer scale.

## Acknowledgements

The authors thank the financial support from the Swiss National Science Foundation, contract No. 200021\_130069 and Sino-Swiss Science and Technology Cooperation (SSSTC), project No. IZLCZ2\_138898.

- [1] a) B. J. Nelson, I. K. Kaliakatsos, J. J. Abbott, *Annu. Rev. Biomed. Eng.* **2010**, *12*, 55–85; b) L. Zhang, K. E. Peyer, B. J. Nelson, *Lab Chip* **2010**, *10*, 2203–2215.
- [2] T. Honda, K. I. Arai, K. Ishiyama, *IEEE Trans. Magn.* **1996**, *32*, 5085–5087.
- [3] D. J. Bell, S. Leutenegger, K. M. Hammar, L. X. Dong, B. J. Nelson, *Proc. IEEE Int. Conf. Rob. Autom.* **2007**, pp. 1128–1133.
- [4] J. J. Abbott, K. E. Peyer, M. C. Lagomarsino, L. Zhang, L. X. Dong, I. K. Kaliakatsos, B. J. Nelson, *Int. J. Robot. Res.* **2009**, *28*, 1434–1447.
- [5] K. Ishiyama, M. Sendoh, A. Yamazaki, K. I. Arai, *Sens. Actuators A* **2001**, *91*, 141–144.
- [6] K. Ishiyama, M. Sendoh, K. I. Arai, *J. Magn. Magn. Mater.* **2002**, *242*, 41–46.
- [7] M. Sendoh, K. Ishiyama, K. I. Arai, *IEEE Trans. Magn.* **2003**, *39*, 3232–3234.
- [8] B. H. McNaughton, J. N. Anker, R. Kopelman, *J. Magn. Magn. Mater.* **2005**, *293*, 696–701.
- [9] A. Ghosh, P. Fischer, *Nano Lett.* **2009**, *9*, 2243–2245.
- [10] T. W. R. Fountain, P. V. Kailat, J. J. Abbott, *IEEE Int. Conf. Rob. Autom.* **2010**, pp. 576–581.
- [11] A. W. Mahoney, J. C. Sarrazin, E. Bamberg, J. J. Abbott, *Adv. Robot.* **2011**, *25*, 1007–1028.
- [12] K. E. Peyer, L. Zhang, B. J. Nelson, *Appl. Phys. Lett.* **2011**, *99*, 174101.
- [13] S. Tottori, L. Zhang, F. Qiu, K. K. Krawczyk, A. Franco-Obregón, B. J. Nelson, *Adv. Mater.* **2012**, *24*, 811–816.
- [14] S. Schuerle, S. Pané, E. Pellicer, J. Sort, M. D. Baró, B. J. Nelson, *Small* **2012**, *8*, 1498–1502.
- [15] S. Jeong, H. Choi, K. Cha, J. Li, J.-o. Park, S. Park, *Sens. Actuators A* **2011**, *171*, 429–435.
- [16] K. Kobayashi, K. Ikuta, *IEEE Int. Conf. Micro Electro Mech. Syst.* **2009**, pp. 11–14.
- [17] E. M. Purcell, *Am. J. Phys.* **1977**, *45*, 3–11.

- [18] a) P. Fischer, A. Ghosh, *Nanoscale* **2011**, 3, 557–563; b) K. E. Peyer, L. Zhang, B. J. Nelson, *Nanoscale* **2012**, DOI: 10.1039/C2NR32554C.
- [19] H. C. Berg, R. A. Anderson, *Nature* **1973**, 245, 380–382.
- [20] C. Bergeles, M. P. Kummer, B. E. Kratochvil, C. Framme, B. J. Nelson, *Medical Image Computing and Computer-Assisted Intervention, Miccai* **2011**, pp. 33–40.
- [21] K. E. Peyer, A. W. Mahoney, L. Zhang, J. J. Abbott, B. J. Nelson in *Microbiorobotics* (Eds.: M. J. Kim, E. B. Steager, A. A. Julius), Elsevier (Amsterdam), **2012**, pp. 165–199.
- [22] M. Sendoh, K. Ishiyama, K. I. Arai, M. Jojo, F. Sato, H. Matsuki, *IEEE Trans. Magn.* **2002**, 38, 3359–3361.
- [23] V. Y. Prinz, V. A. Seleznev, A. K. Gutakovskiy, A. V. Chehovskiy, V. V. Preobrazhenskii, M. A. Putyato, T. A. Gavrilova, *Physica E* **2000**, 6, 828–831.
- [24] O. G. Schmidt, K. Eberl, *Nature* **2001**, 410, 168–168.
- [25] L. Zhang, E. Deckhardt, A. Weber, C. Schonenberger, D. Grutzmacher, *Nanotechnology* **2005**, 16, 655–663.
- [26] a) L. Zhang, J. J. Abbott, L. Dong, B. E. Kratochvil, D. Bell, B. J. Nelson, *Appl. Phys. Lett.* **2009**, 94, 064107; b) L. Zhang, J. J. Abbott, L. Dong, K. E. Peyer, B. E. Kratochvil, H. Zhang, C. Bergeles, B. J. Nelson, *Nano Lett.* **2009**, 9, 3663–3667.
- [27] K. Kobayashi, K. Ikuta, *Appl. Phys. Lett.* **2008**, 92, 262505.
- [28] F. Qiu, S. Tottori, L. Zhang, B. J. Nelson, *Microelectron. Eng.* **2012**, submitted.
- [29] K. E. Peyer, L. Zhang, B. E. Kratochvil, B. J. Nelson, *Proc. IEEE Int. Conf. Rob. Autom.* **2010**, pp. 96–101.
- [30] N. J. Demestre, W. B. Russel, *J. Eng. Math.* **1975**, 9, 81–91.
- [31] M. J. Kim, K. S. Breuer, *Phys. Fluids* **2004**, 16, L78–L81.
- [32] E. Lauga, W. R. DiLuzio, G. M. Whitesides, H. A. Stone, *Biophys. J.* **2006**, 90, 400–412.
- [33] a) T. Petit, L. Zhang, K. E. Peyer, B. E. Kratochvil, B. J. Nelson, *Nano Lett.* **2012**, 12, 156–160; b) L. Zhang, T. Petit, Y. Lu, B. E. Kratochvil, K. E. Peyer, R. Pei, J. Lou, B. J. Nelson, *ACS Nano* **2010**, 4, 6228–6234; c) E. J. Smith, D. Makarov, S. Sanchez, V. M. Fomin, O. G. Schmidt, *Phys. Rev. Lett.* **2011**, 107, 097204.
- [34] A. W. Mahoney, N. D. Nelson, E. M. Parsons, J. J. Abbott, *Proc. IEEE/RSJ Int. Conf. Intell. Rob. Syst.* **2012**, pp. 3559–3564.
- [35] K. E. Peyer, F. Qiu, L. Zhang, B. J. Nelson, *Proc. IEEE/RSJ Int. Conf. Intell. Rob. Syst.* **2012**, pp. 2553–2558.
- [36] T. G. Leong, C. L. Randall, B. R. Benson, N. Bassik, G. M. Stern, D. H. Gracias, *Proc. Natl. Acad. Sci. USA* **2009**, 106, 703–708.
- [37] K. Kikuchi, A. Yamazaki, M. Sendoh, K. Ishiyama, K. I. Arai, *IEEE Trans. Magn.* **2005**, 41, 4012–4014.
- [38] M. J. Kim, K. S. Breuer, *J. Fluids Eng.* **2007**, 129, 319–324.
- [39] S. Martel, C. C. Tremblay, S. Ngakeng, G. Langlois, *Appl. Phys. Lett.* **2006**, 89, 233904.
- [40] a) S. Sánchez, M. Pumera, *Chem. Asian J.* **2009**, 4, 1402–1410; b) A. A. Solovov, W. Xi, D. H. Gracias, S. M. Harazim, C. Deneke, S. Sanchez, O. G. Schmidt, *ACS Nano* **2012**, 6, 1751–1756.
- [41] a) O. Ergeneman, G. Dogangil, M. P. Kummer, J. J. Abbott, M. K. Nazeeruddin, B. J. Nelson, *IEEE Sens. J.* **2008**, 8, 29–37; b) O. Ergeneman, G. Chatzipirpiridis, J. Pokki, M. Marín-Suárez, G. A. Sotiriou, S. Medina-Rodríguez, J. F. Fernández Sánchez, A. Fernández-Gutiérrez, S. Pané, B. J. Nelson, *IEEE Trans. Biomed. Eng.* **2012**, 59, 3104–3109.
- [42] F. Sato, M. Jojo, H. Matsuki, T. Sato, M. Sendoh, K. Ishiyama, K. I. Arai, *IEEE Trans. Magn.* **2002**, 38, 3362–3364.
- [43] F. Qiu, L. Zhang, S. Tottori, K. Marquardt, K. K. Krawczyk, A. Franco-Obregón, B. J. Nelson, *Mater. Today* **2012**, 15, 463.
- [44] M. Peuster, C. Hesse, T. Schloo, C. Fink, P. Beerbaum, C. von Schenkenburg, *Biomaterials* **2006**, 27, 4955–4962.
- [45] a) G. J. Hancock, *Proc. R. Soc. London Ser. A* **1953**, 217, 96–121; b) J. Gray, G. J. Hancock, *J. Exp. Biol.* **1955**, 32, 802–814; c) J. J. L. Higdon, *J. Fluid Mech.* **1979**, 94, 331–351.
- [46] a) S. W. Kim, Y. H. Bae, T. Okano, *Pharm. Res.* **1992**, 9, 283–290; b) C. Lin, A. T. Metters, *Adv. Drug Delivery Rev.* **2006**, 58, 1379–1408.
- [47] a) E. J. Smith, D. Makarov, O. G. Schmidt, *Soft Matter* **2011**, 7, 11309–11313; b) W. Li, G. Huang, H. Yan, J. Wang, Y. Yu, X. Hu, X. Wu, Y. Mei, *Soft Matter* **2012**, 8, 7103–7107.

Published online: November 30, 2012